J|A|C|S ARTICLES

Published on Web 05/22/2009

Application of Solid-State ^{209}Bi NMR to the Structural Characterization of Bismuth-Containing Materials

Hiyam Hamaed,[†] Michael W. Laschuk,[†] Victor V. Terskikh,[‡] and Robert W. Schurko*,[†]

Department of Chemistry and Biochemistry, University of Windsor, Windsor, Ontario, Canada N9B 3P4, and Steacie Institute for Molecular Sciences, National Research Council Canada, Ottawa, Ontario, Canada K1A 0R6

Received February 20, 2009; E-mail: rschurko@uwindsor.ca

Abstract: Herein, we report the first detailed study of ^{209}Bi solid-state NMR (SSNMR) spectroscopy of extremely broad central transition powder patterns. ^{209}Bi ultrawideline SSNMR spectra of several bismuth-containing materials (bismuth oxyhalides, bismuth nitrate pentahydrate, nonaaquabismuth triflate, and bismuth acetate) were acquired at field strengths of 9.4 and 21.1 T using frequency-stepped techniques. The ^{209}Bi SSNMR experiments at 9.4 T yield powder patterns with breadths ranging from 0.9 to 14.6 MHz, from which quadrupolar coupling constants, $C_Q(^{209}\text{Bi})$, between 78 and 256 MHz, were extracted via analytical simulations. The breadths of the quadrupolar-dominated spectra and overall experimental times are greatly reduced for experiments conducted at 21.1 T, which yield high signal-to-noise spectra in which the smaller effects of bismuth chemical shift anisotropy can be clearly observed. The ^{209}Bi electric field gradient (EFG) and chemical shift (CS) tensor parameters extracted from these spectra are correlated to the molecular structures at the bismuth sites, via first principles calculations of ^{209}Bi EFG and CS tensors performed using CASTEP for periodic solids and Gaussian 03 for molecular clusters. The rapidity with which ^{209}Bi SSNMR spectra can be acquired at ultrahigh fields, the sensitivity of the ^{209}Bi NMR parameters to the bismuth environment, and the predictive power of theoretically calculated NMR interaction tensors suggest that ^{209}Bi SSNMR may be useful for the characterization of a variety of Bi-containing materials and compounds.

Introduction

Bismuth is an element rarely found naturally in its pure form; however, it is acquired as a byproduct of lead ore mining and is commonly encountered in bismuth oxides[1,2] and man-made coordination complexes.[3,4] Recently, bismuth-containing compounds have become important in a number of research areas, including synthesis of pharmaceuticals,[5−8] design of superconductors,[2] and catalytic processes.[9] With the increased occurrence in the literature of bismuth-containing systems and associated chemistry and materials science implications, methods of characterizing the structure and bonding at the Bi sites are becoming increasingly important.

While X-ray crystallography is useful for structural determinations in highly crystalline systems, and ^{1}H and ^{13}C NMR experiments are routinely applied for identification of bismuth coordination complexes in solution, characterization of bismuth sites in solid materials has largely been limited to ^{209}Bi nuclear quadrupole resonance (NQR, vide infra).[10−19] ^{209}Bi is the only naturally occurring isotope of bismuth and has a nuclear spin of 9/2. Despite its 100% natural abundance, moderate gyromagnetic ratio and high receptivity with respect to ^{13}C, i.e., $D^{C}(^{209}\text{Bi}) = 848$),[20] ^{209}Bi NMR spectroscopy is very limited because of its large nuclear quadrupole moment (eQ).[21] In all but the most spherically symmetric Bi environments, the

* Author to whom correspondence should be addressed: Phone: (519) 253-3000x3548. Fax: (519) 973-7098.
† University of Windsor.
‡ National Research Council Canada.

(1) Mehring, M. *Coord. Chem. Rev.* **2007**, *251*, 974–1006.
(2) Breunig, H. J. *Kirk-Othmer Encyclo. Chem. Technol. (5th Ed.)* **2004**, *4*, 16–43.
(3) Briand, G. G.; Burford, N. *Adv. Inorg. Chem.* **2000**, *50*, 285–357.
(4) Stavila, V.; Davidovich, R. L.; Gulea, A.; Whitmire, K. H. *Coord. Chem. Rev.* **2006**, *250*, 2782–2810.
(5) Briand, G. G.; Burford, N. *Chem. Rev.* **1999**, *99*, 2601–2657.
(6) Sadler, P. J.; Li, H.; Sun, H. *Coord. Chem. Rev.* **1999**, *185−186*, 689–709.
(7) Yang, N.; Sun, H. *Coord. Chem. Rev.* **2007**, *251*, 2354–2366.
(8) Sun, H.; Sadler, P. J. *Top. Biol. Inorg. Chem.* **1999**, *2*, 159–185.
(9) Hua, R. *Curr. Org. Synth.* **2008**, *5*, 1–27.
(10) Kravchenko, E. A.; Orlov, V. G.; Shlykov, M. P. *Russ. Chem. Rev.* **2006**, *75*, 77–93.
(11) Van der Kelen, G. P.; De Ketelaere, R. F. *J. Mol. Struct.* **1974**, *23*, 329–335.
(12) Zemnukhova, L. A.; Kuznetsov, S. I.; Davidovich, R. L. *Russ. Chem. Bull.* **1998**, *47*, 2169–2172.
(13) Bastow, T. J.; Whitfield, H. J. *J. Magn. Reson.* **1977**, *26*, 461–468.
(14) Kravchenko, E. A.; Kargin, Y. F.; Egorysheva, A. V.; Buslaev, Y. A. *Russ. J. Coord. Chem.* **2001**, *27*, 542–547.
(15) Swiger, E. D.; Green, P. J.; McKown, G. L.; Graybeal, J. D. *J. Phys. Chem.* **1965**, *69*, 949–952.
(16) Buslaev, Y. A.; Kravchenko, E. A.; Pakhomov, V. I.; Skorikov, V. M.; Semin, G. K. *Chem. Phys. Lett.* **1969**, *3*, 455–456.
(17) Kravchenko, E. A.; Morgunov, V. G.; Kargin, Y. F.; Egorysheva, A. V.; Orlov, V. G.; Shlikov, M. P. *Appl. Magn. Reson.* **2004**, *27*, 65–75.
(18) Gopalakrishnan, K. V.; Gupta, L. C.; Vijayaraghavan, R. *Pramana* **1976**, *6*, 343–348.
(19) Brill, T. B.; Long, G. G. *Inorg. Chem.* **1970**, *9*, 1980–1985.
(20) Harris, R. K.; Becker, E. D.; Cabral De Menezes, S. M.; Goodfellow, R.; Granger, P. *Pure Appl. Chem.* **2001**, *73*, 1795–1818.

combination of the large eQ and moderate electric field gradients (EFGs) at the Bi site results in sizeable quadrupolar interactions. These serve to severely broaden ^{209}Bi NMR patterns, and drastically reduce both the T_1 and T_2 relaxation time constants, making routine NMR experimentation very challenging. To date, there are very few ^{209}Bi NMR studies in the literature and no systematic SSNMR study of ^{209}Bi quadrupolar and chemical shift parameters. Reports of ^{209}Bi SSNMR have largely focused on measurement of relaxation time constants and Knight shifts for ^{209}Bi in super- and semiconducting materials[22−29] and on spectra of $BiVO_4$ single crystals.[30,31]

Despite the aforementioned difficulties, there are reasons why ^{209}Bi SSNMR spectroscopy is an attractive technique for structural characterization. ^{209}Bi SSNMR experiments can be very useful for probing the local Bi environments, as well as for increasing the understanding of structures and dynamics at the molecular/atomic level. Notably, ^{209}Bi SSNMR may be especially valuable for characterization of disordered solids or for microcrystalline solids for which crystal structures are unavailable. The ^{209}Bi quadrupolar interaction is important in this regard: the EFGs at the ^{209}Bi nucleus, which arise from the surrounding atoms and bonds, are described by an EFG tensor, which is a symmetric, traceless, second-rank (3 × 3) matrix with three principal components defined as $|V_{33}| \geq |V_{22}| \geq |V_{11}|$. The quadrupolar parameters derived from this tensor are the nuclear quadrupolar coupling constant, $C_Q = eQV_{33}/h$, and the asymmetry parameter, $\eta_Q = (V_{11} - V_{22})/V_{33}$. These parameters are sensitive to both major and minor structural changes, with accurate measurements of C_Q and η_Q providing information on the spherical and axial symmetry, respectively, of the ground-state electronic environments at Bi sites.

Numerous bismuth-containing materials have been studied by ^{209}Bi NQR, often referred to as "zero-field NMR", via measurement of C_Q and η_Q.[10−19] However, ^{209}Bi NQR is very time-consuming, since extremely wide frequency ranges must be swept to detect the frequencies of interest. This could be alleviated somewhat by theoretical computation of ^{209}Bi quadrupolar parameters; unfortunately, reliable computational methods do not currently exist for universally predicting ^{209}Bi EFG tensor parameters with accuracy.

Frequency-stepped NMR techniques have been shown to be very useful for the acquisition of the ultrawideline (UW) NMR spectra for various nuclei in a variety of materials.[32−39] These techniques generally involve stepping the transmitter frequency (at a constant field strength) in even increments, and acquiring individual subspectra with limited excitation bandwidths, which are then coadded or projected to generate the final UWNMR spectrum. The S/N of these spectra can be very low due to their extreme breadths. Timely acquisition of high quality spectra is further exacerbated for nuclei with low natural abundances and/or low gyromagnetic ratios. This has been partially addressed by the application of the quadrupolar Carr−Purcell−Meiboom−Gill NMR (QCPMG) sequence[40] for acquisition of frequency-stepped UWNMR spectra.[39,41] More recently, wideband uniform rate smooth truncation (WURST) echo and QCPMG sequences have been shown to be very effective for rapid spectral acquisition,[42−44] and should be advantageous for the acquisition of high S/N ^{209}Bi UWNMR spectra.

Herein, we demonstrate the effectiveness of ^{209}Bi frequency-stepped UWNMR techniques for the study of a variety of bismuth-containing materials. To the best of our knowledge, there is no methodical ^{209}Bi SSNMR study of this sort reported in the literature to date. A set of well characterized bismuth complexes (i.e., either by NQR and/or single-crystal XRD) with disparate bismuth environments is examined in order to start building a database of ^{209}Bi NMR data, which may have use in future structural studies of bismuth-containing systems. First, the ^{209}Bi SSNMR data for solid BiOX systems (X = Cl, Br, and I), which have well-known quadrupolar parameters obtained from NQR,[13] are presented. Then, ^{209}Bi SSNMR data are shown for some Bi coordination compounds for which ^{209}Bi quadrupolar parameters have not been reported, including bismuth nitrate pentahydrate, nonaaquabismuth triflate, and bismuth acetate. Finally, we discuss a preliminary investigation of theoretical ^{209}Bi quadrupolar and chemical shielding parameters obtained from both plane wave (CASTEP) and ab initio (Gaussian 03) methods.

Experimental Section

Sample Preparation. Samples of BiOI, BiOCl, $Bi(NO_3)_3 \cdot 5H_2O$, and $Bi(OTf)_3$ were purchased from Sigma-Aldrich Canada, Ltd., and used without further modifications. $Bi(CH_3CO_2)_3$ was purchased from Strem Chemicals, Inc. BiOBr was synthesized in our laboratory following slightly modified literature procedures[45] (our sample was heated at 160 °C in an oven for 8 h). Nonaaquabismuth triflate, $[Bi(H_2O)_9](OTf)_3$, was obtained by rehydrating $Bi(OTf)_3$ in air at room temperature (Figure S1, Supporting Information).[46]

(21) Bieron, J.; Pyykko, P. *Phys. Rev. Lett.* **2001**, *87*, 133003/133001–133003/133004.
(22) Dudnik, E. F.; Gene, V. V.; Mnushkina, I. E. *Izv. Akad. Nauk. SSSR, Ser. Fiz.* **1979**, *43*, 1723–1725.
(23) Dupree, R.; Walstedt, R. E. *AIP Conf. Proc.* **1976**, *29*, 350–351.
(24) Dupree, R.; Gardner, J. A. *J. Phys., Colloq.* **1980**, 20–23.
(25) Reyes, A. P.; Heffner, R. H.; Canfield, P. C.; Thompson, J. D.; Fisk, Z. *Phys. Rev. B* **1994**, *49*, 16321–16330.
(26) Reyes, A. P.; Le, L. P.; Heffner, R. H.; Ahrens, E. T.; Fisk, Z.; Canfield, P. C. *Physica B (Amsterdam, Neth.)* **1995**, *206 & 207*, 332–335.
(27) Fukushima, E. *J. Chem. Phys.* **1971**, *55*, 2463–2466.
(28) Flynn, C. P.; Seymour, E. F. W. *Proc. Phys. Soc. London* **1959**, *73*, 945–947.
(29) Morgan, K.; Sayer, B. G.; Schrobilgen, G. J. *J. Magn. Reson.* **1983**, *52*, 139–142.
(30) Lim, A. R.; Choh, S. H.; Jang, M. S. *J. Phys.: Condens. Matter* **1992**, *4*, 1607–1613.
(31) Lim, A. R.; Choh, S. H.; Jang, M. S. *Solid State Commun.* **1996**, *97*, 699–702.
(32) Lipton, A. S.; Wright, T. A.; Bowman, M. K.; Reger, D. L.; Ellis, P. D. *J. Am. Chem. Soc.* **2002**, *124*, 5850–5860.
(33) Sparks, S. W.; Ellis, P. D. *J. Am. Chem. Soc.* **1986**, *108*, 3215–3218.
(34) Medek, A.; Frydman, V.; Frydman, L. *J. Phys. Chem. A* **1999**, *103*, 4830–4835.
(35) Massiot, D.; Farnan, I.; Gautier, N.; Trumeau, D.; Trokiner, A.; Coutures, J. P. *Solid State Nucl. Magn. Reson.* **1995**, *4*, 241–248.
(36) Kennedy, M. A.; Vold, R. L.; Vold, R. R. *J. Magn. Reson.* **1991**, *92*, 320–331.
(37) Bastow, T. J. *Z. Naturforsch., A: Phys. Sci.* **1994**, *49*, 320–328.
(38) Bastow, T. J.; Smith, M. E. *Solid State Nucl. Magn. Reson.* **1992**, *1*, 165–174.
(39) Tang, J. A.; Ellis, B. D.; Warren, T. H.; Hanna, J. V.; Macdonald, C. L. B.; Schurko, R. W. *J. Am. Chem. Soc.* **2007**, *129*, 13049–13065.
(40) Larsen, F. H.; Jakobsen, H. J.; Ellis, P. D.; Nielsen, N. C. *J. Phys. Chem. A* **1997**, *101*, 8597–8606.
(41) Tang, J. A.; Masuda, J. D.; Boyle, T. J.; Schurko, R. W. *ChemPhysChem* **2006**, *7*, 117–130.
(42) Bhattacharyya, R.; Frydman, L. *J. Chem. Phys.* **2007**, *127*, 194503/194501–194503/194508.
(43) O'Dell, L. A.; Schurko, R. W. *Chem. Phys. Lett.* **2008**, *464*, 97–102.
(44) O'Dell, L. A.; Rossini, A. J.; Schurko, R. W. *Chem. Phys. Lett.* **2009**, *468*, 330–335.
(45) Zhang, X.; Ai, Z.; Jia, F.; Zhang, L. *J. Phys. Chem. C* **2008**, *112*, 747–753.
(46) Loueer, M.; Le Roux, C.; Dubac, J. *Chem. Mater.* **1997**, *9*, 3012–3016.

Solid-State NMR. ^{209}Bi SSNMR experiments were carried out on a Varian Infinity Plus spectrometer equipped with a 9.4 T ($\upsilon_0(^1H)$ = 399.73 MHz) Oxford wide-bore magnet at the University of Windsor with $\upsilon_0(^{209}Bi)$ = 65.455 MHz, and a 21.1 T ($\upsilon_0(^1H)$ = 900.08 MHz) Bruker Avance II spectrometer ($\upsilon_0(^{209}Bi)$ = 144.64 MHz) at the National Ultrahigh-field NMR Facility for Solids in Ottawa, Canada. In all cases, NMR powder patterns were too broad to be uniformly excited with a single high-power pulse; hence, spectra were acquired by stepping the transmitter frequency across the entire central transition powder pattern in even increments, collecting the individual subspectra and coadding them to form the total pattern (see Tables S1, S2 for full experimental details).[34,35] In most instances, spectra were acquired using either the Hahn-echo or solid-echo pulse sequences of the forms $(\pi/2)_x$-τ_1-$(\pi)_y$-τ_2-acq and $(\pi/2)_x$-τ_1-$(\pi/2)_y$-τ_2-acq, respectively, where τ represents the interpulse delays. In cases where the T_2 is long enough, experiments at 9.4 T were performed using either the QCPMG[40,47,48] or WURST-QCPMG[43,44] pulse sequences. Bismuth chemical shifts were referenced to a saturated solution of $Bi(NO_3)_3 \cdot 5H_2O$ in concentrated HNO_3 (δ_{iso} = 0.0 ppm).[20] Analytical simulations of ^{209}Bi NMR spectra were performed using WSolids.

Experiments at 9.4 T. Samples were finely ground and packed into either 5 mm o.d. zirconium oxide rotors or 5 mm glass NMR tubes. ^{209}Bi NMR spectra were collected using a Varian 5 mm double-resonance (HX) static probe. For Hahn-echo and QCPMG experiments, a central-transition selective $\pi/2$ pulse width of 0.75 μs (υ_1 = 66.7 kHz) was applied, with an optimized recycle delay of 0.025 s, and spectral widths ranging from 2 to 4 MHz. In the QCPMG experiments, the number of Meiboom−Gill (MG) loops was set to 40. For WURST-QCPMG experiments, a 50 μs WURST pulse length, swept across a range of 2000 kHz at a rate of 40 MHz/ms, was used. The number of echoes was set to 20, the spectral width to 2 MHz, and recycle delay to 0.1 s. In all experiments, the transmitter frequency step size was set between 100 to 150 kHz, in order to ensure uniform excitation. Experimental times ranged from 1 to 14 h, depending upon the pattern breadth, the number of subspectra collected, and the desired S/N.

Experiments at 21.1 T. Samples were ground and packed into 4 mm o.d. zirconium oxide rotors. ^{209}Bi NMR spectra of all samples were acquired with a 4 mm HX MAS probe, using the frequency-stepped Hahn-echo technique described above. All experiments were conducted with a selective $\pi/2$ pulse width of 1 μs (υ_1 = 50.0 kHz), spectral widths of either 2 or 4 MHz, and optimized recycle delays of 0.2 s. Transmitter frequency offsets of 500 kHz were used, and total experimental times ranged from 1 to 14 h. In samples with short T_2* values, the full echo acquisition was often employed to improve the S/N.

Ab Initio Calculations. ^{209}Bi EFG tensor parameters were calculated using both CASTEP software[50] and Gaussian 03.[51] Ab initio plane-wave density functional theory (DFT) calculations for the BiOX (X = Cl, Br, I) series were performed using the CASTEP NMR program[50,52] in the Materials Studio 4.3 environment on an HP xw4400 Workstation with a single Intel Dual-Core 2.67 GHz processor and 8 GB DDR RAM. Ultrasoft pseudopotentials[52] were used for ^{209}Bi EFG calculations with a plane wave basis set cutoff of 610 eV in an ultrafine accuracy basis set with the Monkhorst−Pack k-space grid size of (6 × 6 × 3). The Perdew, Burke, and Ernzerhof (PBE) functionals were used in the generalized gradient approximation (GGA) for the exchange-correlation energy.[53,54] The magnetic shielding tensors for ^{209}Bi were calculated in ultrafine accuracy basis set using the projector-augmented wave method (GIPAW) implemented in the CASTEP code.[55,56] The CIF crystal structure files used in the calculations are from the Crystallography Open Database (COD)[57] and built based on previously published results.[58,59] CASTEP geometry optimization of the BiOX structures did not show any significant changes in the calculated NMR parameters; therefore, only results for nonoptimized structures are presented for clarity (see Supporting Information for further discussion).

Ab initio calculations using Gaussian 03 were performed on bismuth nitrate pentahydrate, nonaaquabismuth triflate, and bismuth acetate on Dell Precision workstations. Atomic coordinates were input from the crystal structures reported in the literature.[60−62] For the first two compounds, calculations were carried out on clusters composed of a central bismuth atom and coordinating organic moieties. However, for bismuth acetate, a larger structural unit was utilized (see Supporting Information for details). In some cases, hydrogen atom positions were geometry optimized using the restricted Hartree−Fock (RHF) method with the 18s15p9d3f (333333/33333/333/3) basis set[63] on the bismuth atom and 3-21G* basis set on lighter atoms (i.e., C, H, O). Calculations of the EFG tensors were performed using both the RHF and B3LYP methods with the 18s15p9d3f (333333/33333/333/3) and 15s12p8d4f (432222/42222/422/4)[63] basis sets on the bismuth atoms and 6-31G* or 6-311G** on the lighter atoms.

Results and Discussion

Solid-State ^{209}Bi NMR. Bismuth Oxyhalides, BiOX (X = I, Br, Cl). The bismuth oxyhalides were chosen for preliminary ^{209}Bi SSNMR experiments since they have high Bi contents and moderate quadrupolar coupling constants (previously determined by NQR to be 91.26, 119.58, and 152.46 MHz for X = I, Br, and Cl, respectively).[13] The ^{209}Bi SSNMR spectra of the BiOX samples and associated simulations are shown in Figure 1, with corresponding NMR parameters summarized in Table 1. The experimental times required to acquire these spectra were relatively short (Tables S1, S2 for details). The spectra reveal that each of these samples has a single chemically distinct bismuth site, in agreement with the crystal structures (Scheme 1). The experimental values of C_Q and η_Q are very close to those determined with NQR,[13] with the values of $C_Q(^{209}Bi)$ increasing with increasing Bi−X interatomic distance. There are larger uncertainties associated with the parameters obtained from NMR experiments than those from NQR due to the wide pattern breadths.

BiOI has the smallest C_Q (91 MHz), and an axially symmetric (η_Q = 0) central transition (CT) pattern with a breadth of ca. 1.1 MHz at 9.4 T. The experimental time for the spectrum

(47) Lipton, A. S.; Bergquist, C.; Parkin, G.; Ellis, P. D. *J. Am. Chem. Soc.* **2003**, *125*, 3768–3772.
(48) Lipton, A. S.; Heck, R. W.; Sears, J. A.; Ellis, P. D. *J. Magn. Reson.* **2004**, *168*, 66–74.
(49) Eichele, K.; Wasylishen, R. E.; *W Solids NMR Simulation Package*, 1.17.30 ed.; Dalhousie University: Halifax, CA, 2001.
(50) Clark, S. J.; Segall, M. D.; Pickard, C. J.; Hasnip, P. J.; Probert, M. I. J.; Refson, K.; Payne, M. C. *Z. Kristallogr.* **2005**, *220*, 567–570.
(51) Frisch, M. J. Gaussian Rev. B.03, Gaussian, Inc., Pittsburgh, 2003.
(52) Profeta, M.; Mauri, F.; Pickard, C. J. *J. Am. Chem. Soc.* **2003**, *125*, 541–548.
(53) Perdew, J. P.; Burke, K.; Ernzerhof, M. *Phys. Rev. Lett.* **1996**, *77*, 3865–3868.
(54) Perdew, J. P.; Burke, K.; Ernzerhof, M. *Phys. Rev. Lett.* **1998**, *80*, 891.
(55) Pickard, C. J.; Mauri, F. *Phys. Rev. B* **2001**, *63*, 245101/245101–245101/245113.
(56) Yates, J. R.; Pickard, C. J.; Mauri, F. *Phys. Rev. B* **2007**, *76*, 024401/024401–024401/024411.
(57) Crystallography Open Database (http://www.crystallography.net/).
(58) Bannister, F. A. *Mineral. Mag. J. Mineral. Soc.* **1935**, *24*, 49–58.
(59) Bannister, F. A. *Nature* **1934**, *134*, 856–857.
(60) Troyanov, S. I.; Pisarevskii, A. P. *Koord. Khim.* **1991**, *17*, 909–913.
(61) Lazarini, F. *Acta Crystallogr., Sect. C: Cryst. Struct. Commun.* **1985**, *C41*, 1144–1145.
(62) Frank, W.; Reiss, G. J.; Schneider, J. *Angew. Chem., Int. Ed. Engl.* **1995**, *34*, 2416–2417.
(63) Huzinaga, S., Ed. *Gaussian Basis Sets for Molecular Calculations*; Elsevier: New York, 1984.

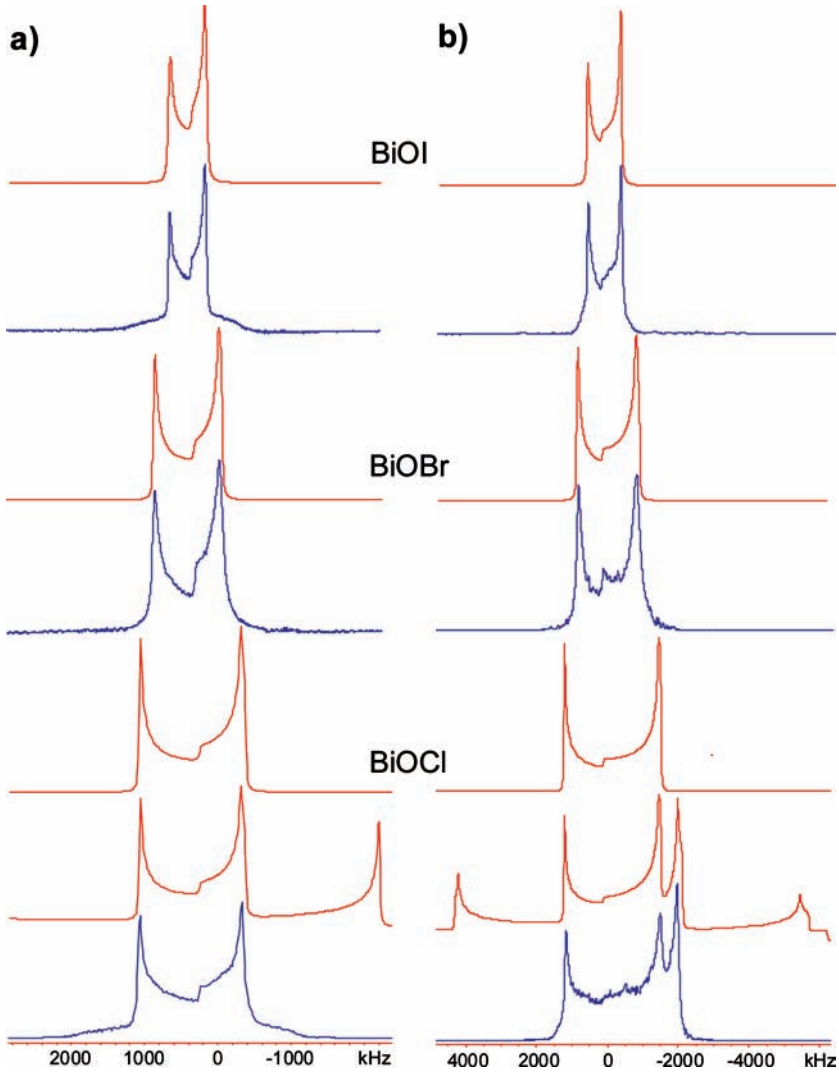

Figure 1. ^{209}Bi SSNMR spectra (blue, experimental; red, simulated) of BiOI, BiOBr, and BiOCl at (a) 21.1 T and (b) 9.4 T. For BiOCl, simulations with and without satellite transitions are shown. The rolling baselines in some of these spectra arise from underlying satellite transitions which have been partially excited.

Table 1. Summary of the Experimental ^{209}Bi NMR Parameters

	$\lvert C_Q(^{209}Bi)\rvert$, MHz[a]	η_Q[b]	δ_{iso}, ppm[c]	Ω, ppm[d]	κ[e]	α, deg[f]	β, deg	γ, deg
BiOI	91(3)	0.01(1)	3200(100)	1100(200)	0.8(2)	0	0	0
BiOBr	122(3)	0.03(3)	3500(200)	2000(300)	0.9(1)	0	2(2)	0
BiOCl	153(3)	0.01(1)	3500(400)	3000(500)	0.9(1)	0	3(3)	0
$Bi(NO_3)_3 \cdot 5H_2O$	78.6(8)	0.66(2)	0(100)	1500(300)	0.7(2)	50(10)	35(5)	95(20)
$Bi(OTf)_3 \cdot 9H_2O$	90(1)	0.01(1)	−750(20)	240(40)	0.6(3)	0	0	0
$Bi(CH_3CO_2)_3$	256(10)	0.30(6)	3200(500)	3400(1000)	0.9(1)	0	2(2)	0

[a] $C_Q = eQV_{33}/h$. [b] $\eta_Q = (V_{11} - V_{22})/V_{33}$. [c] $\delta_{iso} = (\delta_{11} + \delta_{22} + \delta_{33})/3$. [d] $\Omega = \delta_{11} - \delta_{33}$. [e] $\kappa = 3(\delta_{22} - \delta_{iso})/\Omega$. [f] Conventions for the Euler angles are described in the WSolids software package.[49]

acquired at 21.1 T is significantly reduced compared to that at 9.4 T because of both increased sensitivity ($S_+ \propto B_0^2$) and the reduced spectral breadth of ca. 685 kHz. The contributions of the second-order quadrupolar interaction to the CT breadth scale as the inverse of the applied magnetic field, whereas contributions of bismuth chemical shift anisotropy (CSA) are directly proportional to the magnetic field strength; hence, it is possible to make relatively accurate determinations of bismuth CS tensor parameters with NMR data at both fields. The span and skew are found to be $\Omega = 1100$ ppm and $\kappa = 0.8$ (see Table 1 for definitions of these parameters), and the Euler angles indicate that the largest component of the EFG tensor, V_{33}, is coincident with the most shielded component of the CS tensor, δ_{33}. The CS tensor is almost axially symmetric, meaning that δ_{33} is distinct, and $\delta_{11} \approx \delta_{22}$, consistent with both the relative orientation of the CS and EFG tensors and $\eta_Q = 0$. The contribution of the CSA represents only ca. 165 kHz or 24% of the breadth of the total powder pattern (Figure S2); thus, accurate measurement of CS tensors is more challenging for the remainder of the complexes discussed herein, all of which have markedly large values of C_Q and CT patterns dominated by second-order quadrupolar contributions (Figures S3 and S4).

BiOBr and BiOCl have C_Q's of 122 and 153 MHz, respectively, and both possess axially symmetric EFG tensors. In

Scheme 1. (a) A Schematic Representation of the Crystal Structure of BiOCl;[a] (b) Coordination Environment of the Bi Atoms[b]

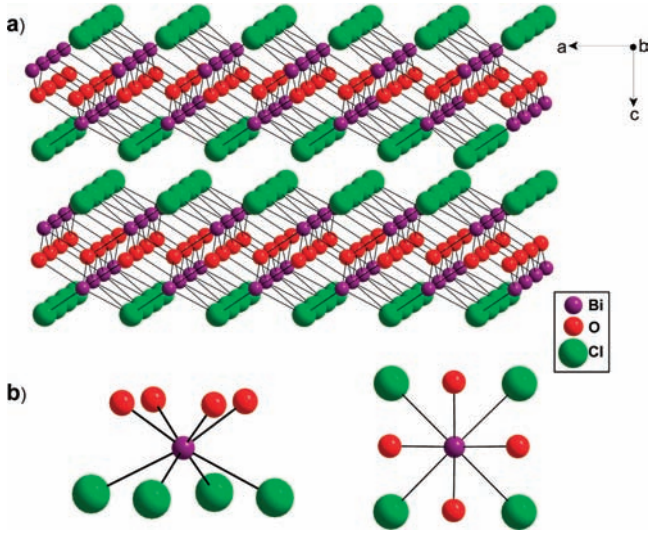

[a] The species in the BiOX series (X = Br, Cl, or I) are isostructural. [b] Consists of a staggered arrangement of four halides and four oxygen atoms (left, side view; right, top view).

addition, the 21.1 T data permits the measurements of effectively axially symmetric CS tensors with significantly larger spans than that of BiOI. Interestingly, in the spectrum of BiOCl, the overlap of the CT and one of the satellite transitions (ST) is observed in the 9.4 T spectrum. The STs for spin-9/2 nuclei are generally "packed" quite tightly about the CT; this foreshadows the increasingly complicated spectra resulting from CT/ST overlaps that are observed for increasing values of C_Q. Traces of the ST patterns are seen on the edges of the CT patterns in all three cases.

It should be mentioned that the Hahn-echo sequence, and not QCPMG, was used for the acquisitions of these spectra because of the extremely short transverse relaxation time constants, T_2, of the ^{209}Bi nuclei. Fitting of CPMG echo intensities as a function of time yielded T_2 values of 97(6) μs, 59(7) μs, and 139(10) μs for BiOI, BiOBr, and BiOCl (Figure S5), respectively. The transverse relaxation is likely to be dominated by the quadrupolar relaxation mechanism; however, unlike in the extreme narrowing limit, there is no clear correlation between the magnitude of C_Q and the value of T_2. It is possible that dipolar relaxation mechanisms may have some influence on the ^{209}Bi T_2 values, since the magnitudes of the ^{209}Bi−X dipolar couplings vary as $R_{DD}(^{209}\text{Bi}, ^{79/81}\text{Br}) > R_{DD}(^{209}\text{Bi}, ^{127}\text{I}) > R_{DD}(^{209}\text{Bi}, ^{35/37}\text{Cl})$, and $T_2(\text{BiOBr}) < T_2(\text{BiOI}) < T_2(\text{BiOCl})$, and the NMR active isotopes are 100% naturally abundant in each case. ^{1}H MAS NMR spectra acquired for each system (not shown) do not reveal significant amounts of proton-containing impurities that could influence the transverse relaxation rates.

Finally, a comment on the bismuth isotropic chemical shifts should be made. While the C_Q is extremely effective at differentiating the Bi environments in these samples, the δ_{iso} is very similar in all three cases (within the large uncertainties), reinforcing the notion that for samples with similar Bi environments, the quadrupolar parameters are crucial for accurate structural characterization. Bismuth chemical shift differences will mainly be useful for differentiating very distinct Bi environments, as noted from previous solution ^{209}Bi NMR studies,[64] and as discussed below.

Bismuth Nitrate Pentahydrate, $Bi(NO_3)_3\cdot 5H_2O$. Previous attempts to obtain a ^{209}Bi NQR signal for $Bi(NO_3)_3\cdot 5H_2O$ were unsuccessful.[12] However, we were able to obtain the ^{209}Bi NMR spectra with relative ease using both the Hahn-echo and the WURST-QCPMG[43] pulse sequences (Figure 2). It is possible to use the QCPMG-type experiments since the T_2 is much longer (1547(35) μs, Figure S6) than those of the BiOX series. The spectrum reveals a powder pattern corresponding to a single bismuth site, in agreement with the crystal structure.[61] The bismuth atom is coordinated by ten oxygen atoms which form an irregular polyhedron composed of four H_2O molecules, two nearly symmetrically bidentate NO_3^- ions (i.e., the Bi−O bond lengths are similar) and one asymmetrically bidentate NO_3^-.[61] Nine of the Bi−O distances range from 2.32 to 2.67 Å and the tenth is 2.99 Å. The smaller C_Q reflects the higher spherical symmetry of the electronic charge distribution about the bismuth atom compared to those in the BiOX systems. In addition, the value of η_Q indicates that the EFG tensor is nonaxially symmetric, which is consistent with the Bi atoms not being positioned on symmetry elements. Since η_Q is nonzero, some minor interference between ST and CT can be seen by comparison of simulations with and without STs (Figure 2).

Nonaaquabismuth Triflate, $[Bi(H_2O)_9](OTf)_3$. Quadrupolar parameters have not previously been obtained for $[Bi(H_2O)_9](OTf)_3$. The ^{209}Bi NMR spectrum (Figure 3) was obtained in a very short time (i.e., about 1 h at 9.4 T) and reveals a powder pattern corresponding to a single bismuth site, again in agreement with the crystal structure.[62] The Bi atom in the nonaaquabismuth cation is coordinated by nine H_2O molecules, with Bi−O distances of 2.448 or 2.577 Å. The slightly larger value of C_Q compared to that of $Bi(NO_3)_3\cdot 5H_2O$ arises from a slightly less spherically symmetric environment and may be due to the smaller bismuth coordination number; however, this is difficult to definitively ascertain without a larger database of quadrupolar parameters and structures for comparison. The cation has a C_{3h} symmetry, which is reflected by the axially symmetric EFG tensor, with V_{33} as its unique component. $Bi(NO_3)_3\cdot 5H_2O$ and $[Bi(H_2O)_9](OTf)_3$ have similar values of δ_{iso}; however, these values are distinct from those of the BiOX series, suggesting that ^{209}Bi nuclei in substantially different environments can be differentiated by chemical shifts extracted from the broad ^{209}Bi SSNMR spectra.

Bismuth Acetate, $Bi(O_2CCH_3)_3$. Bismuth acetate has only one bismuth site in the asymmetric unit, with a coordination environment described as an irregular, nine-vertex polyhedron. The lone electron pair of the bismuth atom occupies a considerable amount of space (i.e., displays stereochemical activity), forcing the bidentate acetato ligands into positions on one side of the Bi atom.[60] As a result, the spherically asymmetric distribution of atoms results in a large quadrupolar interaction, as reflected in the expansive ^{209}Bi NMR pattern (Figure 4).

The spectrum acquired at 9.4 T is extremely broad, requiring the acquisition of 143 QCPMG-subspectra to roughly span the CT and several closely spaced discontinuities from some of the STs. Some of the intensities are inconsistent with the simulation, which could arise from variation in the transverse (T_2) relaxation parameters of the CT and STs, or more likely, differential excitation of the CT and STs (i.e., CTs and STs have distinct

(64) Dixon, K. R. In *Multinuclear NMR*; Mason, J., Ed.; Plenum Press: New York, 1987; p 369.

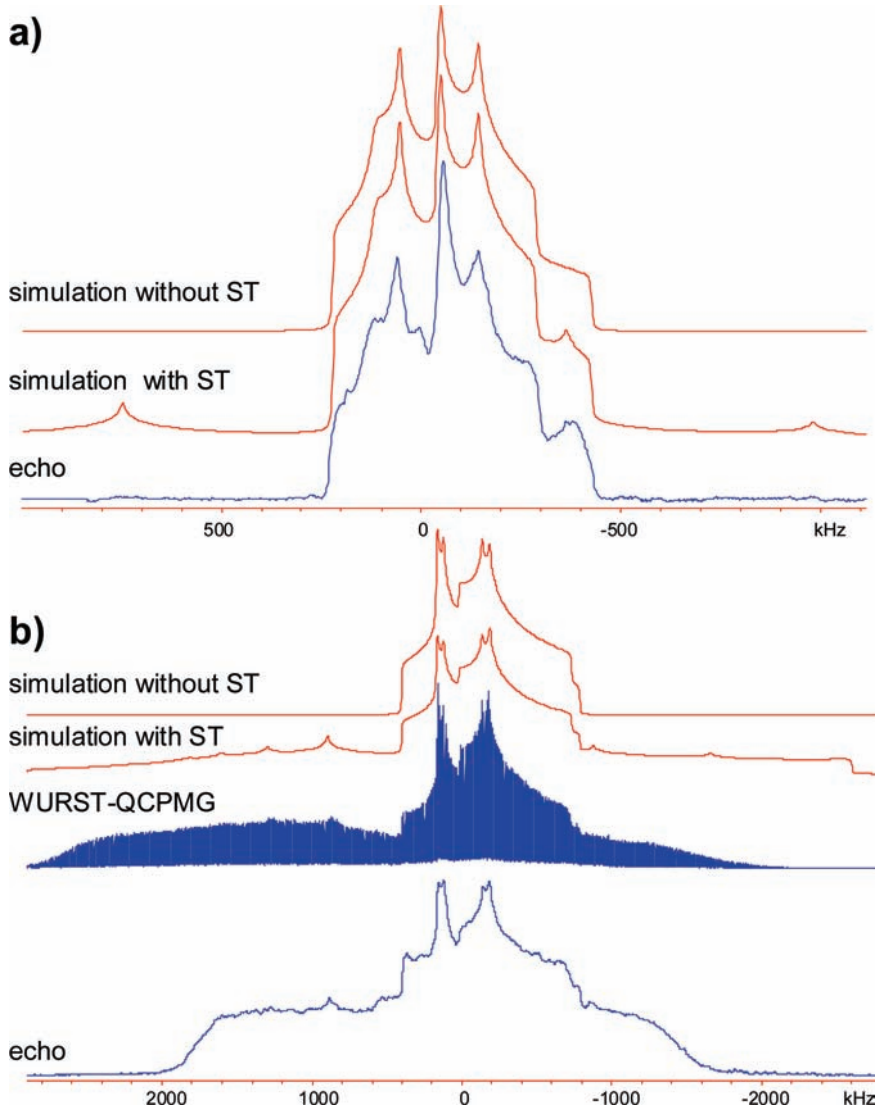

Figure 2. ^{209}Bi SSNMR spectra of bismuth nitrate pentahydrate at (a) 21.1 T and (b) 9.4 T. Not all of the satellite transitions were acquired in order to shorten experimental time, more ST subspectra were acquired in the WURST spectrum because of the shorter experimental time.

nutation rates which can potentially give rise to different relative intensities).[65,66] It is also possible that these discrepancies may arise from the failure of the high field approximation (i.e., $\upsilon_0 \gg \upsilon_Q$), since the C_Q of 256 MHz corresponds to a υ_Q of ca. 10.7 MHz; however, the dominant quantization axis is still the Zeeman axis ($\upsilon_0(^{209}\text{Bi}) = 65.455$ MHz at 9.4 T). In contrast, the spectrum at 21.1 T ($\upsilon_0(^{209}\text{Bi}) = 146.927$ MHz) is constructed from 13 subspectra, and the CT and ST discontinuities match well with simulations, suggesting that the high field approximation holds in this case. The C_Q is much larger than those of the previous samples, because of the influence of the stereochemically active lone pairs of the Bi atom.[60]

We note that the δ_{iso} is similar to that of the BiOX series, despite the distinct Bi chemistry; this can be attributed, in part, to the large errors associated with the measurement of δ_{iso}. There are very few reports of bismuth chemical shifts in the literature available for comparison to our data. Aside from several studies of ^{209}Bi Knight shifts,[22,24−27,29] ^{209}Bi chemical shifts have only been reported for species such as the highly symmetric BiF_6^- anion in acetone,[29] aqueous solutions of bismuth salts, and the $[Bi(H_2O)_6]^{3+}$ cation formed in solutions of $Bi(NO_3)_3$ in concentrated nitric acid.[67] Since the chemical shifts presented herein represent the majority of bismuth chemical shifts reported in the literature, it is difficult to comment further at this time. It is possible that Bi may have a chemical shift range similar to that of antimony, which has been estimated at ca. 3500 ppm.[68]

Theoretical Calculations of ^{209}Bi EFG and CS Tensors. An appreciation of the relationships between solid-state structures and bismuth NMR interaction tensors will be crucial for making future structural interpretations for the multitude of Bi-containing materials. To develop a basis for understanding these relationships, we have conducted ab initio calculations of the ^{209}Bi EFG tensors for all of the systems discussed above, as well as ^{209}Bi CS tensors for the BiOX series. In this section, we present an examination of the principal components and tensor orientations with respect to the molecular coordinates.

(65) Man, P. P. In *Encyclopedia of Analytical Chemistry*; A., M. R., Ed.; J. Wiley: Chichester, 2000; pp 12224−12265.
(66) Man, P. P. *J. Chem. Phys.* **1997**, *106*, 3908–3919.
(67) Fedotov, M. A.; Yukhin, Y. M.; Shubin, A. A.; Udalova, T. A. *Zh. Neorg. Khim.* **1998**, *43*, 307–310.
(68) Dixon, K. R. In *Multinuclear NMR*; Mason, J., Ed.; Plenum Press: New York, 1987; pp 60−61−369.

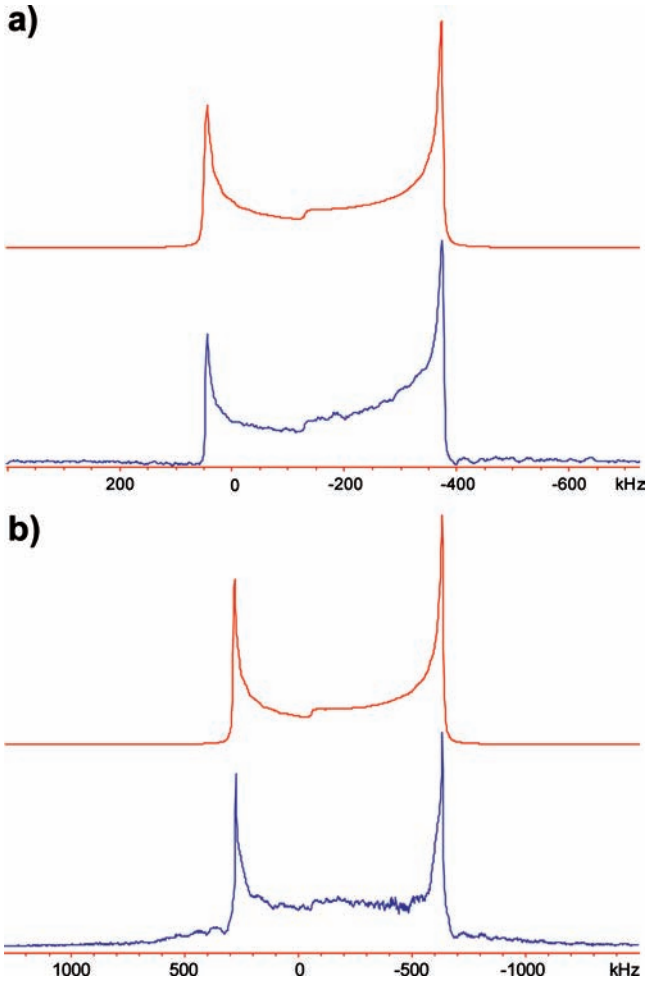

Figure 3. ^{209}Bi SSNMR spectra of nonaaquabismuth triflate at (a) 21.1 T and (b) 9.4 T. The rolling baselines in these spectra arise from underlying satellite transitions which have been partially excited.

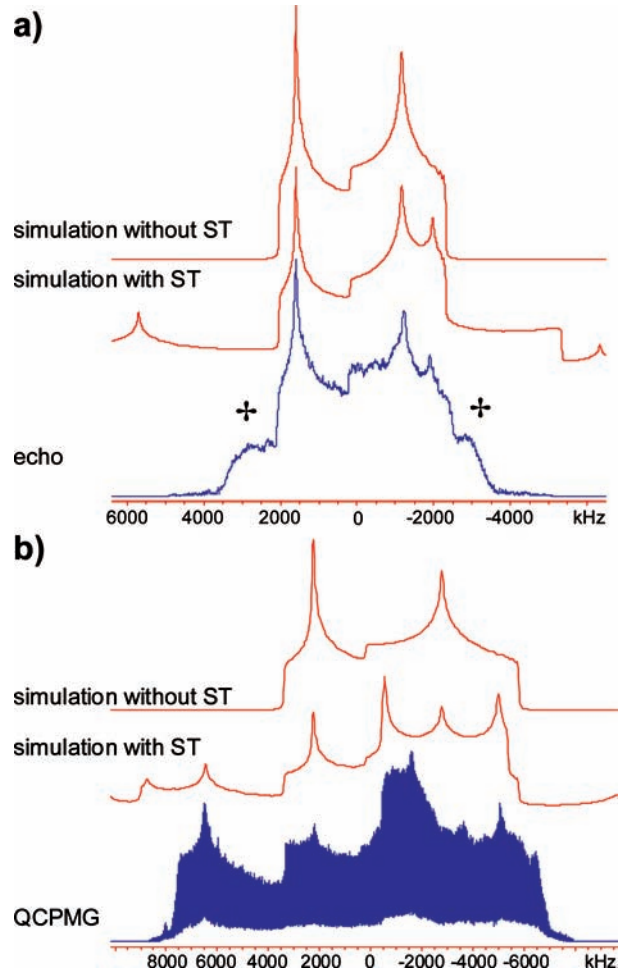

Figure 4. ^{209}Bi SSNMR spectra of bismuth acetate at (a) 21.1 T and (b) 9.4 T. + indicates satellite transition.

Table 2. Comparison of the Experimental and CASTEP ^{209}Bi EFG Tensor Parameters of the BiOX Series

	V_{11}, a.u.	V_{22}, a.u.	V_{33}, a.u.	$C_Q(^{209}Bi)$, MHz[a]	η_Q
BiOI expt	–	–	–	91(3)	0.0
BiOI calcd	0.3381	0.3381	−0.6763	+58.8	0.0
BiOBr expt	–	–	–	122(3)	0.0
BiOBr calcd	0.6067	0.6067	−1.2133	+105.5	0.0
BiOCl expt	–	–	–	153(3)	0.0
BiOCl calcd	0.7402	0.7402	−1.4805	+128.7	0.0

[a] Theoretical values of C_Q ($C_Q = eQV_{33}/h$) are calculated by converting from atomic units to Hz by multiplying V_{33} by $(eQ/h)(9.7177 \times 10^{21}$ V m$^{-2})$, where $Q(^{209}Bi) = -0.37 \times 10^{-28}$ m^2. The absolute values of the experimental C_Q's are reported, while theoretical values are reported with the calculated signs.

CASTEP Calculations for the BiOX Series. Compounds in the BiOX series crystallize in a tetragonal unit cell with the *P*4/*nmm* space group.[58,59] Their structures consist of metal−oxygen layers separated by two halide sheets (Scheme 1). The bismuth atoms are located on special positions, i.e., 4*mm*, and are coordinated by four oxygen atoms and four halide atoms. Because of the periodicity of these structures, CASTEP software[50] was used to calculate the ^{209}Bi EFG parameters. The calculated C_Q's (Tables 2) are consistently lower than the experimental values, and values of η_Q are axially symmetric in all cases. The disagreement between experimental and theoretical C_Q's may arise from either the nature of the Bi pseudopotential (a full investigation of which is beyond the scope of this paper) or the degree of uncertainty in the experimentally measured and theoretically calculated ^{209}Bi nuclear quadrupole moments. Bieroń and Pyykkö have pointed out that values of $Q(^{209}Bi)$ have been put forward that range from −370 to −710 mb,[21] with the most likely candidates being −370(26) mb[69,70] and −500(80) mb.[71] It is clear from the results for the BiOX species (Table 2), and also for the molecular Bi species (Table 4, vide infra), that arbitrary variation in the magnitude of $Q(^{209}Bi)$ could certainly lead to better agreement in some cases, while simultaneously diminishing agreement in others. In this work, we have elected to utilize $Q(^{209}Bi) = -370$ mb (0.37×10^{-28} m^2) for all of our conversions from a.u. to MHz, since there are numerous reports of $Q(^{209}Bi)$ close to this value, and since this provides uniformity in our comparisons of experimental and theoretical data. Nonetheless, the experimental trend of increasing values of C_Q in the series X = I, Br, Cl is replicated.

The CS tensor parameters have also been calculated for the BiOX series (Table 3). We do not report the theoretical isotropic chemical shifts, as a reliable computational reference standard

(69) Raghavan, P. *At. Data Nucl. Data Tables* **1989**, *42*, 189–291.
(70) Lee, W.; Chen, M. Y.; Cheng, S. C.; Macagno, E. R.; Rushton, A. M.; Wu, C. S. *Nucl. Phys. A* **1972**, *181*, 14–24.
(71) Beetz, R.; De Boer, F. W. N.; Panman, J. K.; Konijn, J.; Pavlopoulos, P.; Tibell, G.; Zioutas, K.; Bergstrom, I.; Fransson, K.; et al. *Z. Phys. A* **1978**, *286*, 215–232.

Table 3. Comparison of the Experimental and CASTEP ^{209}Bi CS Tensor Parameters of the BiOX Series

	σ_{11}, ppm	σ_{22}, ppm	σ_{33}, ppm	σ_{iso}, ppm[a]	Ω, ppm[b]	κ[c]	α, deg	β, deg	γ, deg
BiOI expt	–	–	–	–	1100(200)	0.8(2)	0	0	0
BiOI calcd	6279.21	6279.21	7430.62	6663	1151	1.0	0	0	0
BiOBr expt	–	–	–	–	2000(300)	0.9(1)	0	2(2)	0
BiOBr calcd	5689.54	5689.54	6766.67	6049	1077	1.0	0	0	0
BiOCl expt	–	–	–	–	3000(500)	0.9(1)	0	3(3)	0
BiOCl calcd	5699.30	5699.30	6799.32	6066	1100	1.0	0	0	0

[a] $\sigma_{iso} = (\sigma_{11} + \sigma_{22} + \sigma_{33})/3$. [b] Span: $\Omega = \sigma_{33} - \sigma_{11}$. [c] Skew: $\kappa = 3(\sigma_{iso} - \sigma_{22})/\Omega$.

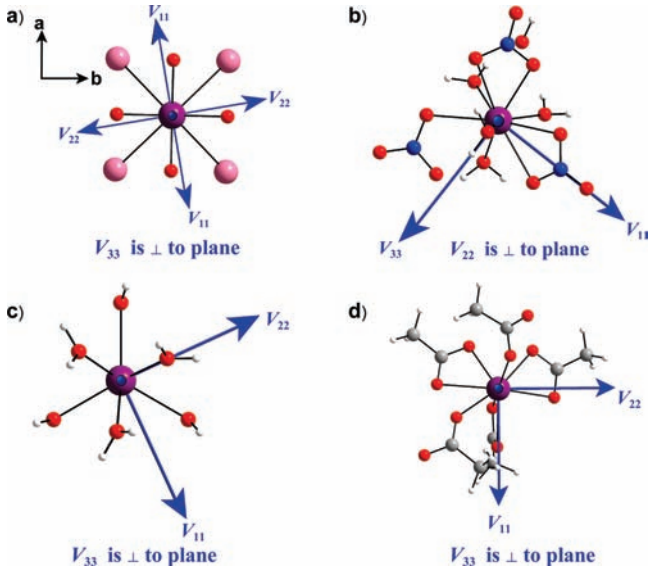

Figure 5. a) ^{209}Bi EFG tensor orientations in (a) BiOX series, (b) $Bi(NO_3)_3 \cdot 5H_2O$, (c) $[Bi(H_2O)_9](OTf)_3$, and (d) $Bi(CH_3CO_2)_3$.

has yet to be established. The theoretical span for BiOI matches very well with experimental data, while those for BiOBr and BiOCl are overestimated. In all cases, the bismuth CS tensors are predicted to be axially symmetric, in good agreement with experiment. The largest component of the EFG tensor, V_{33}, is aligned along the c axis of the unit cell, as expected (Figure 5a), and the V_{11} and V_{22} are consistently oriented slightly askew of the Bi−O bonds ($\angle V_{22}$−Bi−O = 27°); however, given that the $\eta_Q = 0$, the precise orientations of V_{11} and V_{22} are not terribly relevant in this case. Furthermore, the most shielded component of the CS tensor, δ_{33}, is found to be collinear with V_{33}, and the associated Euler angles are in excellent agreement with experiment.

Gaussian 03 Calculations for the Molecular Species. Calculations of the ^{209}Bi EFG tensors on the nonperiodic, molecular systems were performed using Gaussian 03[51] software. The basis sets and methods which are in best agreement with the experiment are discussed separately for each system. Little success was achieved with calculations of ^{209}Bi CS tensors on these species, and hence these results are not discussed at this time.

Both the RHF and B3LYP methods overestimate the values of C_Q for $Bi(NO_3)_3 \cdot 5H_2O$ (Table 4); however, the B3LYP method predicts a nonaxially symmetric tensor, in agreement with experiment. The discrepancy between the experimental and theoretically calculated C_Q may be due to longer range interactions which were not accounted for in the calculations, or possibly deficiencies in the Bi basis sets. The EFG tensor has an unusual orientation, with V_{22} oriented near the molecular pseudo-3-fold axis, and the distinct component, V_{11}, pointing approximately in the direction of one of the bidentate ligands ($\angle$(N−Bi−V_{11}) = 18.4°, Figure 5b).

As for $Bi(NO_3)_3 \cdot 5H_2O$, the calculations on $[Bi(H_2O)_9](OTf)_3$ using the B3LYP method with (333333/33333/333/3) and 6-31G* basis sets yield C_Q and η_Q values in good agreement with the experimental values, suggesting that the Bi basis set may indeed be suitable for such calculations, and/or that longer-range influences on the ^{209}Bi EFG tensor are less significant in this molecule. V_{33} is the unique component of the EFG tensor and is oriented along the C_3 axis (Figure 5c), akin to the orientations of metal EFG tensors in $Co(acac)_3$ and $Al(acac)_3$.[72,73] V_{11} and V_{22} are identical, as indicated by $\eta_Q = 0$.

For $Bi(CH_3CO_2)_3$, calculations performed on small clusters (i.e., structural units with one bismuth atom and coordinated acetate ligands, see Figure S7) yield values of C_Q and η_Q that are in poor agreement with experiment. Since bismuth acetate has a polymeric structure,[60] a larger cluster consisting of three bismuth atoms and nine acetate ligands was used. For this larger cluster, the RHF calculations predict C_Q and η_Q values in good agreement with experiment, and further increasing the size of the structural unit to include seven bismuth atoms and eighteen acetate ligand produces even better agreement. These data are much better than those from similar B3LYP calculations; however, it is unclear why the RHF calculations are superior in this instance. The RHF calculation, performed on the largest structural unit with the RHF method and the (333333/33333/333/3) and 6-31G* basis sets (Table 4), predicts a nearly axially symmetric tensor, with the distinct V_{33} component oriented close to the shortest Bi−O bond ($\angle$(V_{33}−Bi−O) = 159°) (Figure 5d).

Conclusions

This is the first detailed account of solid-state ^{209}Bi NMR spectroscopy of broad central and satellite transition powder patterns. Frequency-stepped techniques have been shown to be very useful for the acquisition of extremely broad ^{209}Bi NMR patterns. Acquisition of ^{209}Bi NMR spectra at 9.4 T is possible, but is predicted to become increasingly inconvenient for the many systems with larger values of C_Q(^{209}Bi). However, acquisition of ^{209}Bi NMR spectra at 21.1 T is much more rapid and should enable the investigation of an enormous array of Bi-containing materials and compounds, providing both quadrupolar and chemical shift data. For extremely large C_Q's, it is possible that ^{209}Bi SSNMR at 21.1 T or higher may be utilized to acquire UW "histogram" spectra[74] to provide rough estimates of quadrupolar parameters, thereby improving the efficiency of complementary ^{209}Bi NQR experiments, which could then be conducted to refine these parameters in very short time frames. Work in this area is currently underway in our laboratory.

(72) Schurko, R. W.; Wasylishen, R. E.; Foerster, H. *J. Phys. Chem. A* **1998**, *102*, 9750–9760.
(73) Eichele, K.; Chan, J. C. C.; Wasylishen, R. E.; Britten, J. F. *J. Phys. Chem. A* **1997**, *101*, 5423–5430.
(74) Bowers, G. M.; Kirkpatrick, R. J. *J. Magn. Reson.* **2007**, *188*, 311–321.

Table 4. Comparison of the Experimental and Gaussian ^{209}Bi EFG Tensor Parameters[a]

method	basis sets (Bi, other atoms)[b]	V_{11}, a.u.	V_{22}, a.u.	V_{33}, a.u.	$C_Q(^{209}Bi)$, MHz[c]	η_Q
			$Bi(NO_3)_3 \cdot 5H_2O$			
experimental	–	–	–	–	78.6(8)	0.66(2)
RHF	A, 6-31G*	−0.5317	−0.5654	1.0972	−95.4	0.03
RHF	B, 6-31G*	−0.5362	−0.5815	1.1178	−97.2	0.04
RHF	A, 6-311G**	−0.5610	−0.5933	1.1544	−100.4	0.03
B3LYP	A, 6-31G*	−0.1720	−0.9953	1.1674	−101.5	0.70
B3LYP	A, 6-311G**	−0.2088	−1.0300	1.2388	−107.7	0.66
			$[Bi(H_2O)_9](OTf)_3$			
experimental	–	–	–	–	90(1)	0.01(1)
RHF	A, 6-31G*	0.3997	0.4030	−0.8027	+69.8	0.00
RHF	A, 6-311G**	0.3925	0.3955	−0.7881	+68.5	0.00
B3LYP	A, 6-31G*	0.4692	0.4782	−0.9474	+82.4	0.00
B3LYP	A, 6-311G**	0.4584	0.4664	−0.9248	+80.4	0.00
			$Bi(CH_3CO_2)_3$			
experimental	–	–	–	–	256(10)	0.30(6)
RHF[d]	A, 6-31G*	−0.3146	−0.9511	1.2658	−110.0	0.50
RHF[d]	A, 6-311G**	−0.3959	−0.9680	1.3639	−118.6	0.42
RHF[e]	A, 6-31G*	−1.2690	−1.8692	3.1383	−272.8	0.19
RHF[e]	A, 6-311G**	−1.3431	−1.8929	3.2361	−281.3	0.17
B3LYP[e]	A, 6-31G*	−0.9307	−1.1102	2.0410	−177.4	0.09
B3LYP[e]	A, 6-311G**	−0.9920	−1.1195	2.1115	−183.6	0.06
RHF[f]	A, 6-31G*	−1.1677	−1.7945	2.9622	−257.5	0.21
RHF[f]	A, 6-311G**	−1.2365	−1.7755	3.0120	−261.9	0.18
B3LYP[f]	A, 6-31G*	−0.8791	−1.1977	2.0768	−180.6	0.15
B3LYP[f]	A, 6-311G**	−0.9341	−1.1875	2.1217	−184.4	0.12

[a] Definitions of parameters are given in Table 2. [b] A and B denote the basis sets (333333/33333/333/3) and (432222/42222/422/4), respectively. [c] The absolute values of the experimental C_Q's are reported while the theoretical values are reported with the calculated signs. [d] Calculations conducted on a cluster consisting of a single bismuth atom and coordinated acetate ligands (Supporting Information). [e] Calculations conducted on a cluster consisting of three bismuth atoms and nine acetate ligands (Supporting Information). [f] Calculations conducted on a cluster consisting of seven bismuth atoms with eighteen acetate ligands (Supporting Information).

The ^{209}Bi quadrupolar interaction dominates the shapes and breadths of the NMR patterns; however, extraction of the quadrupolar parameters is relatively straightforward, even in cases where there is overlap between the CT and STs. The quadrupolar parameters and (to a lesser degree) isotropic chemical shifts reflect the geometry, symmetry, and coordination environment of the bismuth atom. Theoretical calculations of the ^{209}Bi EFG and CS tensor parameters are in reasonably good agreement with the experimental values and will help in structural predictions for which crystallographic data are not available. Clearly, our work suggests that some further effort is required on the development of suitable basis sets for bismuth, as well as on the refinement of the value of $Q(^{209}Bi)$. Finally, the ^{209}Bi EFG and CS tensor orientations within the atomic coordinate systems/molecular frames provide us with a starting point for the rationalization of the origin of these tensors and their correlations to molecular structure and symmetry. We hope that this work encourages future ^{209}Bi NMR and NQR studies on the ever expanding catalog of Bi-containing systems.

Acknowledgment. R.W.S. thanks the Natural Science and Engineering Research Council (NSERC) for supporting this research. R.W.S. also acknowledges the Ontario Ministry of Research and Innovation for support in the form of an Early Researcher Award. We thank the Canadian Foundation for Innovation (CFI), the Ontario Innovation Trust (OIT), the University of Windsor and NSERC for funding of the solid-state NMR centre at the University of Windsor, and the Centre for Catalysis and Materials Research (CCMR) at Windsor for additional support. H.H. thanks the Ministry of Training, Colleges and Universities for an Ontario Graduate Scholarship and UW for a Tuition Scholarship. M.L. thanks NSERC for an undergraduate summer research award (USRA). Dr. Luke O'Dell is thanked for his help with the WURST-QCPMG experiment, and Mr. Aaron Rossini is acknowledged for helpful comments on this project. Access to the 900 MHz NMR spectrometer was provided by the National Ultrahigh-Field NMR Facility for Solids (Ottawa, Canada), a national research facility funded by CFI, OIT, Recherche Québec, the National Research Council Canada, and Bruker BioSpin and managed by the University of Ottawa (www.nmr900.ca). NSERC is acknowledged for a Major Resources Support grant.

Supporting Information Available: Complete ref 51, powder XRD data, and experimental details are available free of charge via the Internet at http://pubs.acs.org.

JA901347K